




Utility of 3T single-voxel proton MR spectroscopy for differentiating intracranial meningiomas from intracranial enhanced mass lesions

Acta Radiologica Open
10(4) 1–10
© The Foundation Acta
Radiologica 2021
Article reuse guidelines:
sagepub.com/journals-permissions
DOI: 10.1177/20584601211009472
journals.sagepub.com/home/arr


Eiji Matsusue¹ , Chie Inoue¹, Sadaharu Tabuchi²,
Hiroki Yoshioka², Yuichiro Nagao², Kensuke Matsumoto¹,
Kazuhiko Nakamura¹ and Shinya Fujii³ 

Abstract

Background: Proton magnetic resonance spectroscopy (MRS) provides structural and metabolic information that is useful for the diagnosis of meningiomas with atypical radiological appearance. However, the metabolite that should be prioritized for the diagnosis of meningiomas has not been established.

Purpose: To evaluate the differences between the metabolic peaks of meningiomas and other intracranial enhanced mass lesions (non-meningiomas) using MR spectroscopy in short echo time (TE) spectra and the most useful metabolic peak for discriminating between the groups.

Material and Methods: The study involved 9 meningiomas, 22 non-meningiomas, intracranial enhancing tumors and abscesses, and 15 normal controls. The ranking of the peak at 3.8 ppm, peak at 3.8 ppm/Creatine (Cr), β - γ Glutamine-Glutamate (bgGlx)/Cr, N-acetyl compounds (NACs)/Cr, choline (Cho)/Cr, lipid and/or lactate (Lip-Lac) at 1.3 ppm/Cr, and the presence of alanine (Ala) were derived. The metabolic peaks were compared using the Mann-Whitney U test. ROC analysis was used to determine the cut-off values for differentiating meningiomas from non-meningiomas using statistically significant metabolic peaks.

Results: The ranking of the peak at 3.8 ppm among all the peaks, peak at 3.8 ppm/Cr, bgGlx/Cr, Lip-Lac/Cr, and the presence of Ala discriminated meningiomas from non-meningiomas with moderate to high accuracy. The highest accuracy was 96.9% at a threshold value of 3 for the rank of the peak at 3.8 ppm.

Conclusion: A distinct elevated peak at 3.8 ppm, ranked among the top three highest peaks, allowed the detection of meningiomas.

Keywords

Magnetic resonance imaging, magnetic resonance spectroscopy, meningioma, 3.8 ppm, short TE

Received 10 March 2021; accepted 23 March 2021

Introduction

Meningiomas are common intracranial neoplasms and arise from the arachnoid cap cells of the leptomeninges. The neoplasms account for approximately 13–40% of intracranial neoplasms, making them the second most common intracranial tumors in adults with an incidence of 1.5–5.5 per 100,000.^{1,2} Currently, the majority of meningiomas are evaluated preoperatively using conventional MRI with gadolinium-DTPA enhancement. However, 15% of meningiomas exhibit atypical MRI features such as ring-like enhancement and parenchymal invasion, resembling malignant brain

¹Department of Radiology, Tottori Prefectural Central Hospital, Tottori, Japan

²Department of Neurosurgery, Tottori Prefectural Central Hospital, Tottori, Japan

³Division of Radiology, Department of Multidisciplinary Internal Medicine, Tottori University, Tottori, Japan

Corresponding author:

Eiji Matsusue, Department of Radiology, Tottori Prefectural Central Hospital, 730 Ezu, Tottori 680-0901, Japan.

Email: matsusuee@tp-ch.jp



lesions such as gliomas or metastatic brain tumors.³⁻⁵ Advanced MRI techniques, including diffusion weighted imaging (DWI), susceptibility-weighted imaging (SWI), perfusion-weighted imaging (PWI), and proton magnetic resonance spectroscopy (MRS), provide specific physiologic information that is not available by conventional MRI alone.^{3,6-8}

Proton MRS studies of meningiomas have shown an increase in alanine (Ala), glutamate (Glu) –glutamine (Gln) complex (Glx) and choline (Cho) and a decrease in N-acetylaspartate (NAA), creatine (Cr), myoinositol (mI) and lipid (Lip).⁹⁻¹³ Ala has been shown to be characteristic for intracranial meningiomas,^{11,14} although several meningiomas lack the Ala.^{9,13,15-19} Glx are also commonly present in meningiomas. The resonance peaks of Glx are contributed from its α , β , and γ proton groups, respectively. Several reports demonstrated elevation of Glx in meningiomas compared to other brain masses.^{13,16,20-22} However, Ala and Glx concentrations are not always easy to evaluate during clinical practice.¹⁸ Peak at 3.8 ppm on short TE spectra has also been demonstrated as a distinct metabolic feature for the differentiation of meningiomas among other cerebral lesions.^{13,15-17,20,23} As for NAA, several authors have mentioned that meningiomas may have endogenous N-acetyl compounds (NACs) except for NAA and may produce an elevated peak around 2.02 ppm.^{15,17} Thus, there are several metabolites for the diagnosis of meningiomas, although it remains unclear which metabolite should be prioritized for the diagnosis of this tumors.

We performed a retrospective study to evaluate differences between meningiomas and other intracranial enhanced mass lesions in metabolic peaks using MRS in short TE spectra and to assess the most useful metabolite peak for discrimination between the groups.

Material and Methods

Patients

In this retrospective study, from January 2014 and January 2021, 60 patients having intracranial mass

lesions showing gadolinium enhancement on T1-weighted images and evaluated on MR spectroscopy in short echo time (TE) spectra were identified. A total of histologically confirmed 31 patients were analyzed in this study; the remaining 29 patients were excluded due to no histological confirmation (24 patients) or inadequate MRS examinations (5 patients). Nine of the 31 patients were diagnosed with meningiomas. Twenty-two of the 31 patients were diagnosed with other tumors (non-meningiomas). The non-meningiomas included brain abscess (n=4), primary central nervous system lymphoma (PCNSL) (n=2), adenocarcinoma (n=5), glioblastoma multiforme (GBM) (n=5), anaplastic astrocytoma (n=1), anaplastic oligodendroglioma (n=1), anaplastic ependymoma (n=1), hemangiopericytoma (n=2), and schwannoma (n=1). Also, normal controls of the contralateral brain showing normal brain were evaluated in 15 of 31 patients. The demographics and histology of meningiomas, non-meningiomas, and normal controls are shown in Table 1.

Our hospital's institutional review board approved this study, and the requirement for written informed consent was waived by the review board due to the retrospective nature of the study.

Image acquisition

MR imaging in all 31 patients and 15 normal controls was performed using the 3-Tesla MR system (Philips Ingenia, Best, The Netherlands) with an eight-channel phased-array head coil, following the standard protocol for adult brain imaging at our hospital: pre- and post-contrast gadolinium-enhanced T1-weighted fast-spoiled gradient echo sequence, TR/TE, 7.0/2.4 ms; slice thickness, 0.7 mm; FOV, 240 × 240 mm; matrix, 360 × 354; T2-weighted fast spin-echo sequence, TR/TE, 4000/85 ms; section thickness, 5 mm; FOV, 240 × 220 mm; matrix, 380 × 270; FLAIR image, TR/TE/IR, 10,000/120/2200; section thickness, 5 mm; FOV 240 × 180 mm; matrix, 320 × 170; and axial spin-echo single-shot echo-planar sequence (DWI), TR/TE, 4400/68 ms; slice thickness, 5 mm; FOV, 240 × 212 mm;

Table 1. Demographics and histology of meningiomas, non-meningiomas, and normal controls.

	Meningiomas	Non-meningiomas	Normal controls
Number	9	22	15
Age (years), mean ± SD	56 ± 17	62 ± 16	64 ± 16
Female/male	6/3	8/14	6/9
Histology	Grade I (7) Grade II (2)	Brain abscess (4), PCNSL (2), AC (5), GBM (5), AA (1), AO (1), AE (1), hemangioblastoma (2), Schwannoma (1)	

PCNSL: primary central nervous system lymphoma; AC: adenocarcinoma; GBM: glioblastoma multiforme; AA: anaplastic astrocytoma; AO: anaplastic oligodendroglioma; AE: anaplastic ependymoma.

matrix, 170×128 . DWI was performed using b values of 0 and 1000 s/mm^2 . Apparent diffusion coefficient (ADC) maps were calculated from the DWI.

Proton MR spectra were acquired after contrast administration in all cases. Single-voxel MRS (TR/TE = 2000/36; 128 averages) was performed. Automated shimming and water suppression methods were used. Signal contamination from fat tissue in the skull and skull base was prevented by using spatially localized saturation bands to suppress the signal from the scalp or orbital fat on MRS. The acquisition time for spectroscopic imaging studies varied between 7 and 10 min. For all MRS acquisitions, the volume of interest (VOI) was manually placed to mainly include the enhancing portions of the lesions on contrast-enhanced axial T1-weighted images. The volume of the VOI was adapted to the size and extent of the lesion, resulting in voxel sizes ranging from $1.1 \times 1.1 \times 1.1$ to $2.1 \times 2.1 \times 2.1 \text{ cm}^3$. None of the cases received mannitol at the time of MRS.

Image analysis

Review of MRS studies was performed by a single experienced neuroradiologist (E.M.). Pre- and post-contrast T1-weighted, T2-weighted, FLAIR and diffusion-weighted images, clinical and histopathological findings were accessible during analysis of MRS data. The following peaks were measured: peak at 3.8 ppm; Cho at 3.21 ppm; Cr at 3.02 ppm; NACs at 2.02 ppm; Ala at 1.48 ppm; bgGlx at 2.1–2.5 ppm; Lip at 1.3 ppm; lactate (Lac) at 1.33 ppm. In this study, Lip and Lac were recorded as Lip and/or Lac (Lip-Lac) because lipids usually overlap with lactate. The peak heights of the metabolites were used in determining the ratios. The relative quantity of each metabolite was measured as the ratio of its peak height to the peak height of creatine. For the metabolite peak at 3.8 ppm, the ranking of the peak at 3.8 ppm among all the peaks was also determined.

Statistical analysis

The Mann-Whitney U test was used to analyze the differences between meningiomas and non-meningiomas, as well as meningiomas and normal controls, for the seven metabolic parameters: the ranking of the peak at 3.8 ppm, peak at 3.8 ppm/Cr, Cho/Cr, NACs/Cr, bgGlx/Cr, Lip-Lac/Cr, and presence of Ala. Finally, we selected the statistically useful metabolic parameters for further analysis.

For the differentiation of meningiomas from non-meningiomas, the cutoff values that provided the best combination of sensitivity and specificity for each adapted metabolic parameter were selected using

receiver operating characteristic (ROC) analysis. The cutoff values were determined using the Youden index. We determined the accuracy, sensitivity, specificity, positive predictive value, and negative predictive value of each parameter using chi-squared analysis. The area under the ROC curve (AUC) of each parameter was also evaluated. $P < 0.01$ was considered indicative of a statistical significance.

All the statistical analyses were performed with EZR (Saitama Medical Center, Jichi Medical University, Saitama, Japan), which is a graphical user interface for R (The R Foundation for Statistical Computing, Vienna, Austria).²⁴

Results

Nine cases of meningioma were characterized by prominent Cho and peak at 3.8 ppm. Cr was reduced in eight cases and distinct in one case. All the cases revealed distinct NACs at 2.02 ppm and bgGlx at 2.1–2.5 ppm. Lip-Lac was distinct in eight cases with meningiomas, whereas it was the prominent peak in one case with atypical meningioma. Ala was present in six of nine cases of meningioma. A summary of the MRS findings for the meningiomas is shown in Table 2. Representative MR images of meningiomas with corresponding spectra are shown in Figs. 1 and 2.

Among 22 cases with non-meningiomas, the peak at 3.8 ppm was visible in 15 of 22 cases and undetectable in the remaining 7 cases, including one PCNSL, one abscess, two adenocarcinomas, two GBMs, and one anaplastic oligodendroglioma. Cr was not visible in four cases, including one abscess, one adenocarcinoma, one hemangioblastoma, and one Schwannoma. Cho was undetectable in two cases, including one abscess and one hemangioblastoma. bgGlx was invisible in five cases, including two abscesses, one adenocarcinoma, one hemangioblastoma, and one schwannoma. NACs at 2.02 ppm were not visible in two cases, including one abscess and one adenocarcinoma. Lip-Lac levels were increased in all 22 cases. MR images of non-meningiomas with the corresponding spectra are shown in Figs. 3 to 5.

In the 15 normal controls, the spectra revealed peaks of NACs, bgGlx, Cr, and Cho and a peak at 3.8 ppm. Only two controls showed a small Lac-Lip. No Ala was visible in any of the normal controls. A representative MR image of the normal control with its corresponding spectrum is shown in Fig. 6.

The seven metabolic parameters, including the ranking of the peak at 3.8 ppm, peak at 3.8 ppm/Cr, Cho/Cr, NACs/Cr, bgGlx/Cr, Lip-Lac/Cr, and the presence of Ala in meningiomas, non-meningiomas, and normal controls, are shown in Table 3. Scatterplots of the six

Table 2. Summary of MRS findings for the meningiomas.

Case	Age/sex	Histology	Location	Ranking of 3.8 ppm	3.8 ppm /Cr	Cho /Cr	NACs /Cr	bgGlx/Cr	Lip-Lac /Cr	Ala
1	73/M	Meningothelial Grade I	Temporal base	2nd	2.77	3.8	1.92	1.38	1.64	+
2	43/M	transitional Grade I	Convexity	2nd	3.62	4.5	2.41	1.76	2.07	+
3	68/F	atypical Grade II	Convexity	3rd	3	7.41	3.61	2.57	6.11	+
4	73/F	fibrous Grade I	Posterior fossa	2nd	2.41	3.16	1.64	1.08	1.3	-
5	55/F	transitional Grade I	Falx	2nd	1.44	2.87	0.68	0.6	0.74	+
6	68/F	fibrous Grade I	Posterior fossa	2nd	3.25	4.25	2.5	1.75	1.88	+
7	36/M	meningothelial Grade I	frontal base	2nd	2.03	1.69	1.92	1.52	1.23	+
8	25/F	atypical Grade II	posterior fossa	2nd	2.87	1.95	2.32	1.44	1.59	-
9	61/F	fibrous Grade I	Posterior fossa	3rd	1.55	3.34	1.95	1.29	1.24	-

3.8 ppm: peak at 3.8 ppm; Cr: creatine; Cho: choline; NACs: N-acetyl compounds; bgGlx: β - γ Glutamine-Glutamate; Lip-Lac: lipid and/or lactate.

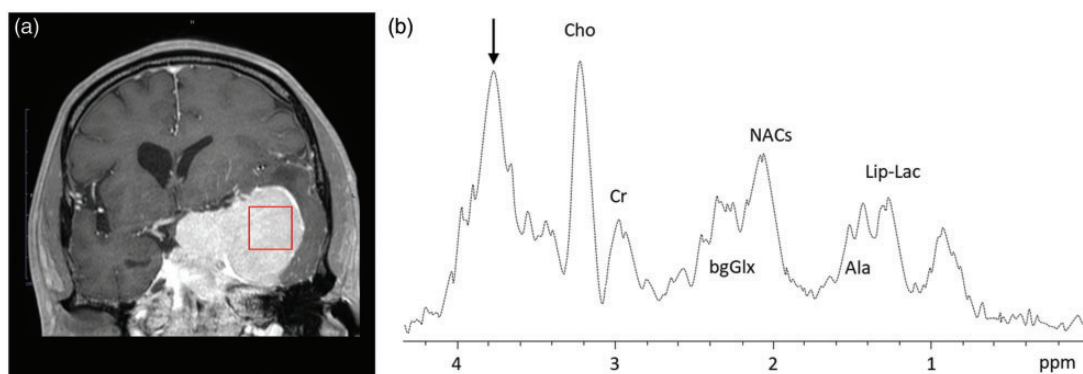


Fig. 1. A representative MR image of meningioma with its corresponding spectrum in case 1. (a) A coronal Gd-enhanced T1-weighted image of meningioma at left temporal base. (b) The spectrum from the VOI shown in (a). Prominent Cho and peak at 3.8 ppm (arrowed) are seen. The ranking of the peak at 3.8 ppm is the second. The peak at 3.8 ppm/Cr ratio, 2.77, Cho/Cr ratio, 3.8, NACs/Cr ratio, 1.92, bgGlx/Cr ratio, 1.38, and Lip-Lac/Cr ratio, 1.64. Ala showing doublet is also seen at 1.48 ppm.

metabolic parameters, except the presence of Ala, are also shown in Fig. 7.

Regarding the peak at 3.8 ppm, the ranking of the peak at 3.8 ppm was the second or third for the meningiomas, the third to seventh for the non-meningiomas, and the fifth to seventh for the normal controls. For the meningiomas, seven cases ranked second (Fig. 1) and two cases ranked third (Fig. 2). For the non-meningiomas, six cases ranked less than the fifth; one case of PCNSL ranked the third (Fig. 3), and two cases of GBM (Fig. 4), one case of anaplastic ependymoma, and two cases of brain abscess (Fig. 5) ranked the fourth. Significant differences were observed between

meningiomas and non-meningiomas ($P < 0.001$), as well as meningiomas and normal controls ($P < 0.001$).

Regarding the other metabolic parameters, significant differences were observed between meningiomas and non-meningiomas for the peak at 3.8 ppm/Cr ($P < 0.001$), bgGlx/Cr ($P < 0.01$), Lip-Lac/Cr ($P < 0.01$), and the presence of Ala ($P < 0.001$). No significant difference was observed between meningiomas and non-meningiomas for NACs/Cr ($P = 0.04$) and Cho/Cr ($P = 0.08$). We adapted statistically useful metabolic parameters, except NACs/Cr and Cho/Cr.

The results of the diagnostic tests for the adapted five metabolic parameters for differentiating

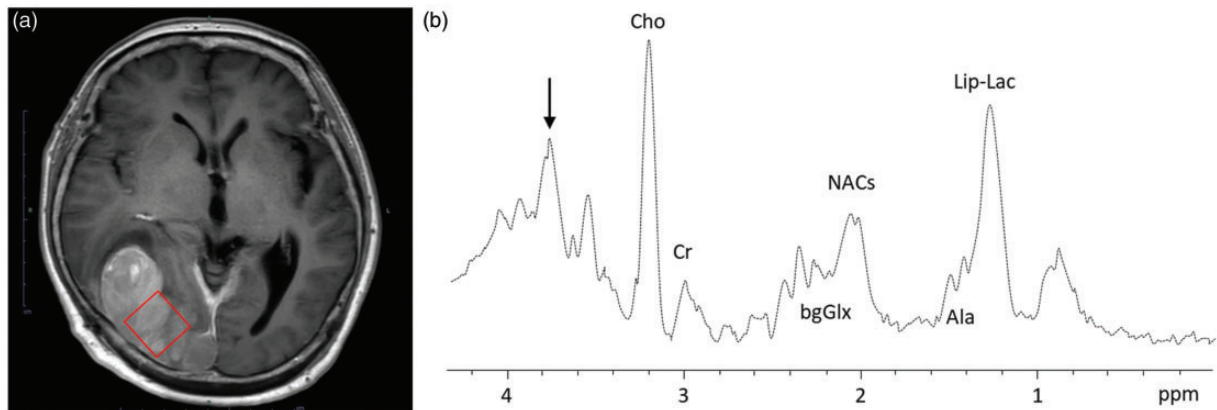


Fig. 2. A representative MR image of meningiomas with its corresponding spectrum in case 3. (a) An axial Gd-enhanced T1-weighted image of meningioma at right temporo-occipital convexity. (b) The spectrum from the VOI shown in (a). Prominent Cho, Lip-Lac at 1.3 ppm and the peak at 3.8 ppm (arrowed) are seen. The ranking of the peak at 3.8 ppm is the third. The peak at 3.8 ppm/Cr ratio, 3.02, Cho/Cr ratio, 7.41, NACs/Cr ratio, 3.61, bgGlx/Cr ratio, 2.57, and Lip-Lac/Cr ratio, 6.11. Small Ala showing doublet is also seen at 1.48 ppm.

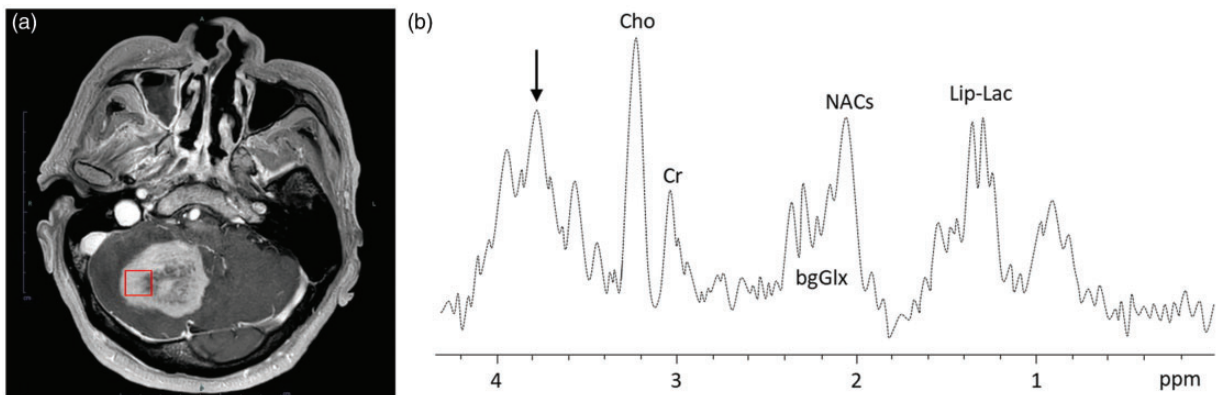


Fig. 3. An MR image of PCNSL with its corresponding spectrum mimicking meningiomas. (a) An axial Gd-enhanced T1-weighted image of PCNSL at right cerebellar hemisphere. (b) The spectrum from the VOI shown in (a). Prominent Cho, NACs and peak at 3.8 ppm are seen. Ranking of the peak at 3.8 ppm is the third ranking. The peak at 3.8 ppm/Cr ratio, 1.52, Cho/Cr ratio, 2.54, NACs/Cr ratio, 1.77, bgGlx/Cr ratio, 1.15, and Lip-Lac/Cr ratio, 1.36. No Ala is seen.

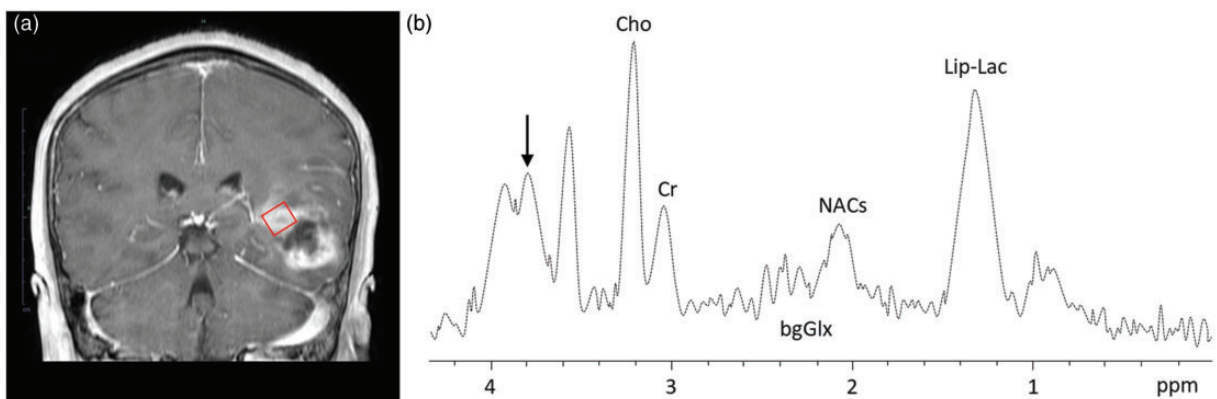


Fig. 4. A representative MR image of GBM with its corresponding spectrum. (a) A coronal Gd-enhanced T1-weighted image of GBM at left temporal lobe. (b) The spectrum from the VOI shown in (a). Prominent Cho and Lip-Lac are seen. The ranking of the peak at 3.8 ppm is the fourth. The peak at 3.8 ppm/Cr ratio, 1.14, Cho/Cr ratio, 2.78, NACs/Cr ratio, 0.84, bgGlx/Cr ratio, 0.52 and Lip-Lac/Cr ratio, 1.94. No Ala is seen.

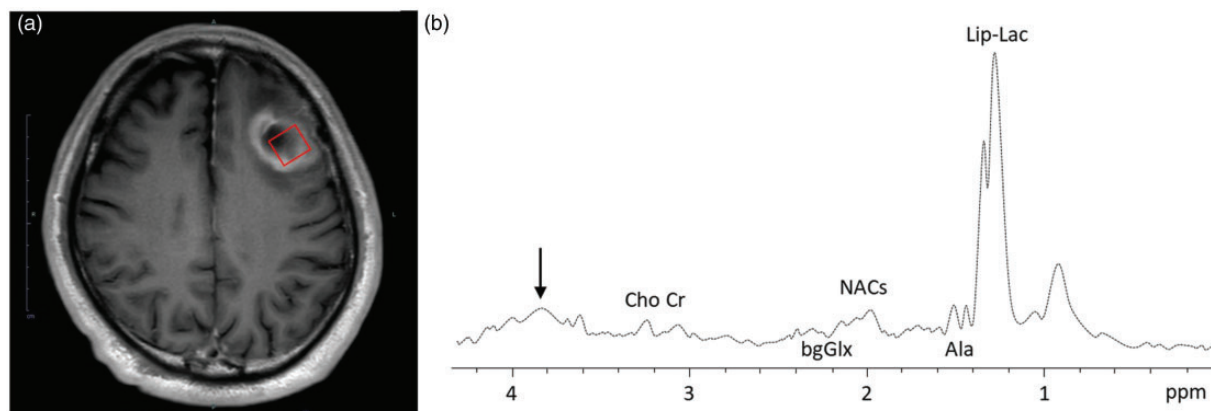


Fig. 5. A representative MR image of brain abscess with its corresponding spectrum. (a) An axial Gd-enhanced T1-weighted image of brain abscess at left frontal lobe. (b) The spectrum from the VOI shown in (a). Prominent Lip-Lac and small Ala showing doublet is seen. A small peak at 3.8 ppm (arrowed) ranks fourth.

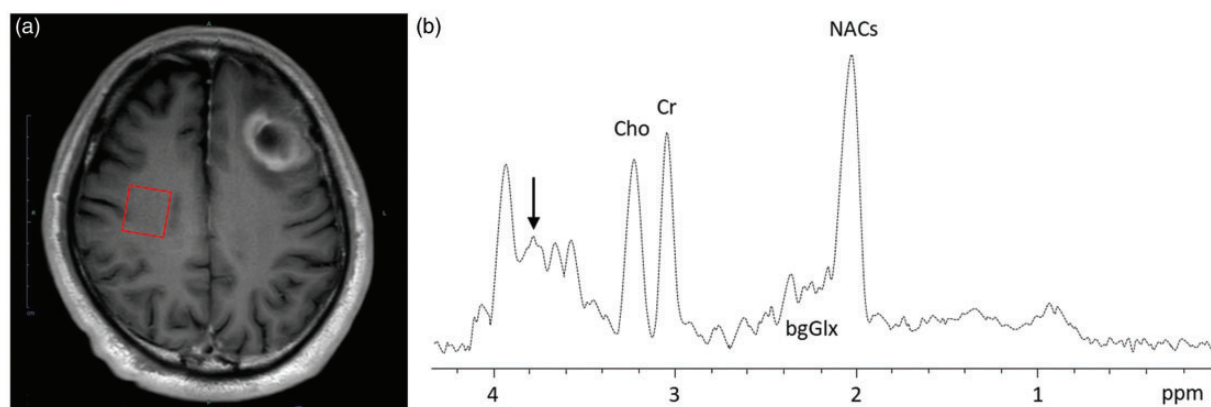


Fig. 6. A representative MR image of the normal control with its corresponding spectrum. (a) An axial Gd-enhanced T1-weighted image of brain abscess at left frontal lobe, same as Fig. 5(a). VOI is placed at the normal contralateral (right) fronto-parietal lobe. (b) The spectrum from the VOI shown in (a). Prominent NACs, Cr, and Cho are seen. The ranking of the peak at 3.8 ppm (arrowed) is the fifth. The peak at 3.8 ppm/Cr ratio, 0.43, Cho/Cr ratio, 0.83, NAA/Cr ratio, 1.36, bgGlx/Cr ratio, 0.28, and Lip-Lac/Cr ratio, 2.07. No Lip-Lac and Ala are seen.

Table 3. The metabolic parameters in meningiomas, non-meningiomas, and normal controls.

Metabolic factors	Meningiomas (9 cases) range (median)	Non-meningiomas (22 cases) range (median)	P ^a	Normal controls (15 cases) range (median)	P ^b
The ranking of 3.8 ppm	2–3 (2)	3–7 (5)	<0.001	5–7 (7)	<0.001
3.8 ppm/Cr	1.44–3.62 (2.77)	0.41–2.11 (1.14)	<0.001	0.2–0.47 (0.35)	<0.001
Cho/Cr	1.69–7.41 (3.34)	0.7–12.57 (2.57)	0.08	0.66–1.12 (0.93)	<0.001
NACs/Cr	0.68–3.61 (1.95)	0.75–2.93 (1.51)	0.04	0.99–1.59 (1.36)	<0.001
bgGlx/Cr	0.6–2.57 (1.44)	0.3–2.6 (0.8)	<0.01	0.18–0.29 (0.24)	<0.001
Lip-Lac/Cr	0.74–6.11 (1.59)	0.3–30.12 (5.99)	<0.01	0.17–0.22 (0.2)	0.02
Ala	6/9	2/21	<0.001	0/15	<0.001

3.8: peak at 3.8 ppm; Cr: creatine; Cho: choline; NACs: N-acetyl compounds; bgGlx: β - γ Glutamine-Glutamate; Lip-Lac: lipid and/or lactate; Ala: alanine.

^aMeningiomas vs. 21 non-meningiomas.

^bMeningioma vs. 15 normal controls.

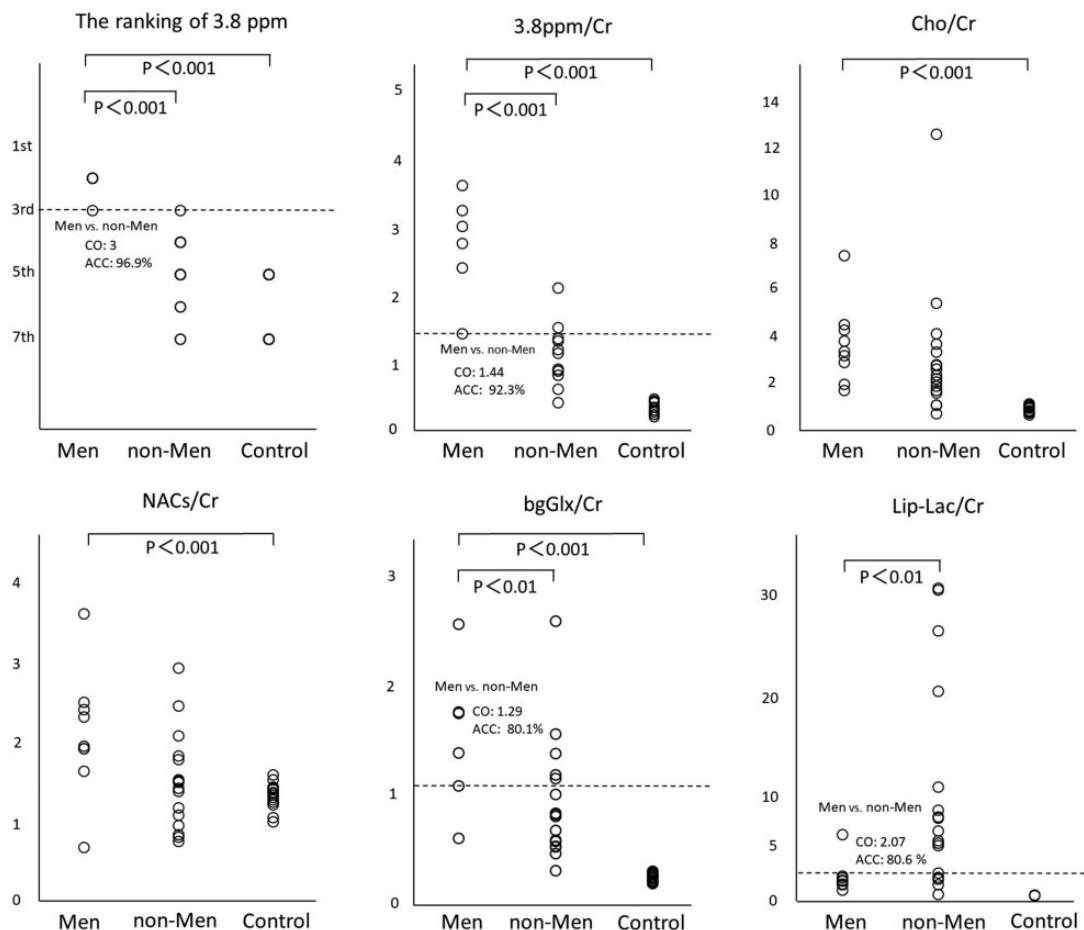


Fig. 7. Scatterplots of the ranking of the peak at 3.8 ppm, the peak at 3.8ppm/Cr, Cho/Cr, NACs/Cr, bgGlx/Cr and Lip-Lac/Cr. Note: 3.8 ppm indicates the peak at 3.8 ppm. Cr: creatine; Cho: choline; NACs: N-acetyl compounds; bgGlx: β - γ Glutamine-Glutamate; Lip-Lac: lipid and/or lactate; Men: meningioma; non-Men: non-meningioma; CO: cutoff value; ACC: accuracy, AI: asymmetry index; SBR: specific binding ratio.

Table 4. The diagnostic tests for the adapted five metabolic parameters for differentiating meningiomas from non-meningiomas.

	AUC	ACC	SEN	SPE	PPV	NPV	P value
The Ranking of 3.8 ppm \leq 3	0.99	96.9%	100%	93.8%	94.2%	100%	<0.001
3.8 ppm/Cr \geq 1.44	0.96	92.3%	100%	84.6%	86.7%	100%	<0.001
Lip-Lac/Cr \leq 2.07	0.82	80.6%	88.9%	72.2%	76.2%	86.7%	<0.001
bgGlx/Cr \geq 1.29	0.82	80.1%	77.8%	82.4%	80.5%	78.5%	<0.001
Ala	0.79	78.8%	66.7%	90.9%	88%	73.2%	<0.001

3.8 ppm: peak at 3.8 ppm; AUC: area under the curve; ACC: accuracy; SEN: sensitivity; SPE: specificity; PPV: positive predictive value; NPV: negative predictive value; Cr: creatine; Lip-Lac: lipid and/or lactate; bgGlx: β - γ Glutamine-Glutamate; Ala: alanine.

meningiomas from non-meningiomas are summarized in Table 4. The highest accuracy was 96.9% at a cutoff value of 3 for the ranking of the peak at 3.8 ppm. The second highest accuracy was 92.3% at a cutoff value of 1.44 for the peak at 3.8 ppm/Cr. The third highest accuracy was 80.6% at a cutoff value of 2.07 for Lip-Lac/Cr. The fourth highest accuracy was 80.1% at a cutoff value of 1.29 for bgGlx/Cr. The lowest accuracy was 78.8% for the presence of Ala.

Discussion

The present study evaluated the metabolic features of meningiomas that would distinguish them from other intracranial enhanced mass lesions using MRS in short TE spectra. The analysis showed a good test accuracy for differentiating meningiomas from non-meningiomas using statistically useful metabolic parameters. The highest accuracy was 96.9% at a threshold value of

3 for the ranking of the peak at 3.8 ppm. Therefore, a distinct elevated peak at 3.8 ppm, ranked among the top three highest peaks, allowed the detection of meningiomas.

An elevated peak at 3.8 ppm was observed in meningiomas, non-meningiomas, and normal controls. We used the “ranking” as a simple objective indicator of peak height at 3.8 ppm. The ranking of the peak at 3.8 ppm was the second or third for meningiomas, the third to seventh for non-meningiomas, and the fifth to seventh for normal controls. There are several metabolites at 3.8 ppm, including leucine, alanine, α -Glx, glutathione, lysine, arginine, serine, guanidinoacetate, phosphoethanolamine, oligosaccharide, trehalose, glucose, and mannitol.^{23,25} In meningiomas, it was evident that all cases revealed a distinct signal at 3.8 ppm, showing the second or third ranking peak. This finding was characteristic, and it differentiated them from other cerebral lesions, obviously due to the underlying metabolic differences. As metabolites at a peak at 3.8 ppm for meningiomas, α -CH amino acids, including α -Glx and glutathione, phosphoethanolamine, oligosaccharide, or guanidinoacetate, have been postulated,^{12,13,16,17,20,23,26} although the chemical substance observed at 3.8 ppm is still undetermined. As for non-meningiomas, a distinct peak at 3.8 ppm has been found in medulloblastomas, germinomas,²⁷ tuberculomas,²⁵ and fungal abscesses,^{28,29} although the metabolite remained unclear in those lesions. In the present study, an important observation is that one case of PCNSL revealed a distinct signal at 3.8 ppm, showing the third ranking peak. To the best of our knowledge, a distinct signal at 3.8 ppm in PCNSL has not been previously reported. As for the normal controls, the metabolite for the peak at 3.8 ppm may have been α -Glx, which is usually seen as a doublet or triplet at 3.65 to 3.8 ppm.³⁰

The evaluation of tumors by MRS usually involves the analysis of Lac and Lip. Lac is the product of anaerobic glycolysis, and Lip is correlated with the extent of microscopic cellular necrosis.^{31,32} Lip is observed to be minimal in typical meningiomas^{11,13,17,22,33} but marked in Schwannomas, metastatic tumors, brain abscesses, and glioblastomas.^{13,34} The present study showed that Lip–Lac/Cr was significantly lower in meningiomas than in non-meningiomas, confirming the findings of the previous studies. Only one case of an atypical meningioma showed prominent Lip–Lac. This finding seemed to indicate microscopic necrosis in atypical meningioma.^{33,35} Yue et al. reported that Lip represents not only micronecrosis in non-benign meningiomas but also microcystic changes or fatty degeneration in benign meningiomas.¹⁷

The bgGlx are spread over the range of 2.1–2.5 ppm and merge with NACs at 2.02 ppm. Several studies

have revealed a higher occurrence of Glx in meningiomas than in other intracranial tumors.^{13,21,22,36} Regarding the assumed metabolic pathways of Glx in meningiomas, Glu is utilized through the transamination and the oxidation of pyruvate. The deamination of Gln to Glu, via glutaminase, could provide Glu for Ala production.¹⁶ In this study, all cases of meningiomas revealed distinct bgGlx. In addition, a significant difference related to bgGlx/Cr was observed between meningiomas and non-meningiomas. Hazany et al. indicated that the peak heights of bgGlx over the range of 2.1–2.5 ppm may facilitate the underestimation of their quantity in the brain.²⁰ Quantitative 1H-MRS studies would be a better measure, as it revealed an increased Glx concentration in meningiomas compared with other intracranial tumors.^{16,21,22}

Ala has been suggested by various studies to underlie meningioma, but it is found in abscesses^{37,38} and rarely in other intracranial tumors.^{12,19,21,39–42} Ala is thought to be an alternative reduced partner of pyruvate derived from glycolysis.²³ Ala is affected by the J-coupling effect and splits as doublets. In this study, the Ala doublet was present in six of nine meningiomas and two of four abscesses. For meningiomas, the frequency of the presence of Ala varies with studies, ranging from 32 to 100%.⁹ Voxel size has been suggested as a factor underlying the variance of Ala.¹⁷ In the present study, all Ala-positive cases had a sufficient voxel size, confirming the report by the study of Yue et al.¹⁷ Hence, Ala is a unique marker of intracranial meningiomas, although its concentration may be underestimated when compared with the observed elevated peak at 3.8 ppm in meningiomas.

Regarding NACs, all cases of meningioma revealed a distinct peak at 2.02 ppm, although no significant difference related to NACs/Cr was observed between meningiomas and non-meningiomas. The important observation is the presence of a distinct peak at 2.02 ppm for meningiomas. NAA is a marker metabolite for neurons, and it can be assumed that the spectra obtained from voxels placed entirely within the meningiomas contained no NAA. Therefore, it should be considered that a peak around 2.02 ppm for meningiomas represents other endogenous NACs, such as N-acetylaspartylglutamate, N-acetylneuraminic acid and N-acetylgalactosamine¹⁷ or short TE metabolites such as bgGlx.

Our study has several limitations. First, this study was carried out in a single hospital; thus, the study population was small. In addition, only nine meningiomas were reviewed, and this was a retrospective study. Second, only short TE spectra were obtained in this study. It is preferable to obtain both short and long TE spectra for the analysis of intracranial lesions. Third, this study was qualitative, and it used ratios of

peak heights to measure the levels of brain metabolites. Quantitative inspection and the use of advanced models for the evaluation of ratios are desirable. Because of these limitations, further validation with a greater number of cases is needed. Allowing for these limitations, we believe our findings provide helpful insights related to the diagnostic workup for meningiomas. Furthermore, this simple evaluation, involving ranking the peak at 3.8 ppm, is expected to be a useful indicator for differentiating meningiomas from intracranial mass lesions in clinical settings.

In conclusion, prominent peak at 3.8 ppm, minimal Lip/Lac, distinct bgGlx and the presence of Ala are metabolic features that can be used to distinguish meningiomas from non-meningiomas. A distinct elevated peak at 3.8 ppm, ranked among the top three highest peaks, facilitated the detection of meningiomas.

Acknowledgements

We are grateful for the expert assistance from the members of the Department of Radiological Technology, Tottori Prefectural Central Hospital.

Declaration of Conflicting Interests


The author(s) declared no potential conflicts of interest with respect to the research, authorship, and/or publication of this article.

Funding

The author(s) received no financial support for the research, authorship, and/or publication of this article.

ORCID iDs

Eiji Matsusue  <https://orcid.org/0000-0002-0411-1600>

Shinya Fujii  <https://orcid.org/0000-0002-0048-0396>

References

- Pereira BJA, de Almeida AN, Paiva WS, et al. Natural history of intraventricular meningiomas: systematic review. *Neurosurg Rev* 2020;43:513–523.
- Claus EB, Bondy ML, Schildkraut JM, et al. Epidemiology of intracranial meningioma. *Neurosurgery* 2005;57:1088–1095; discussion 1088–1095.
- Huang RY, Bi WL, Griffith B, et al. Imaging and diagnostic advances for intracranial meningiomas. *Neuro Oncol* 2019;21:i44–i61.
- Hakyemez B, Yildirim N, Erdoğan C, et al. Meningiomas with conventional MRI findings resembling intraaxial tumors: can perfusion-weighted MRI be helpful in differentiation? *Neuroradiology* 2006;48:695–702.
- Harting I, Hartmann M, Bonsanto MM, et al. Characterization of necrotic meningioma using diffusion MRI, perfusion MRI, and MR spectroscopy: case report and review of the literature. *Neuroradiology* 2004;46:189–193.
- Chen T, Jiang B, Zheng Y, et al. Differentiating intracranial solitary fibrous tumor/hemangiopericytoma from meningioma using diffusion-weighted imaging and susceptibility-weighted imaging. *Neuroradiology* 2020; 62:175–184.
- Siempis T, Tsakiris C, Alexiou GA, et al. Diagnostic performance of diffusion and perfusion MRI in differentiating high from low-grade meningiomas: a systematic review and meta-analysis. *Clin Neurol Neurosurg* 2020;190:105643.
- Soares DP, Law M. Magnetic resonance spectroscopy of the brain: review of metabolites and clinical applications. *Clin Radiol* 2009;64:12–21.
- Chernov MF, Kasuya H, Nakaya K, et al. (1)H-MRS of intracranial meningiomas: what it can add to known clinical and MRI predictors of the histopathological and biological characteristics of the tumor? *Clin Neurol Neurosurg* 2011;113:202–212.
- Sibtain NA, Howe FA, Saunders DE. The clinical value of proton magnetic resonance spectroscopy in adult brain tumours. *Clin Radiol* 2007;62:109–119.
- Demir MK, Iplikcioglu AC, Dincer A, et al. Single voxel proton MR spectroscopy findings of typical and atypical intracranial meningiomas. *Eur J Radiol* 2006;60:48–55.
- Majós C, Julià-Sapé M, Alonso J, et al. Brain tumor classification by proton MR spectroscopy: comparison of diagnostic accuracy at short and long TE. *AJNR Am J Neuroradiol* 2004;25:1696–1704.
- Cho Y-D, Choi G-H, Lee S-P, et al. 1H-MRS metabolic patterns for distinguishing between meningiomas and other brain tumors. *Magn Reson Imaging* 2003;21:663–672.
- Gill SS, Thomas DG, Van Bruggen N, et al. Proton MR spectroscopy of intracranial tumours: in vivo and in vitro studies. *J Comput Assist Tomogr* 1990;14:497–504.
- Kousi E, Tsougos I, Fountas K, et al. Distinct peak at 3.8 ppm observed by 3T MR spectroscopy in meningiomas, while nearly absent in high-grade gliomas and cerebral metastases. *Mol Med Rep* 2012;5:1011–1018.
- Crisi G. (1)H MR spectroscopy of meningiomas at 3.0T: the Role of glutamate-glutamine complex and glutathione. *Neuroradiol J* 2011;24:846–853.
- Yue Q, Isobe T, Shibata Y, et al. New observations concerning the interpretation of magnetic resonance spectroscopy of meningioma. *Eur Radiol* 2008;18:2901–2911.
- Howe FA, Barton SJ, Cudlip SA, et al. Metabolic profiles of human brain tumors using quantitative in vivo 1H magnetic resonance spectroscopy. *Magn Reson Med* 2003;49:223–232.
- Kinoshita Y, Yokota A. Absolute concentrations of metabolites in human brain tumors using in vitro proton magnetic resonance spectroscopy. *NMR Biomed* 1997;10:2–12.
- Hazany S, Hesselink JR, Healy JF, et al. Utilization of glutamate/creatine ratios for proton spectroscopic diagnosis of meningiomas. *Neuroradiology* 2007;49:121–127.
- Majós C, Alonso J, Aguilera C, et al. Proton magnetic resonance spectroscopy ((1)H MRS) of human brain tumours: assessment of differences between tumour

- types and its applicability in brain tumour categorization. *Eur Radiol* 2003;13:582–591.
22. Majós C, Alonso J, Aguilera C, et al. Utility of proton MR spectroscopy in the diagnosis of radiologically atypical intracranial meningiomas. *Neuroradiology* 2003;45:129–136.
 23. Tugnoli V, Schenetti L, Mucci A, et al. Ex vivo HR-MAS MRS of human meningiomas: a comparison with in vivo ¹H MR spectra. *Int J Mol Med* 2006;18:859–869.
 24. Kanda Y. Investigation of the freely available easy-to-use software ‘EZR’ for medical statistics. *Bone Marrow Transplant* 2013;48:452–458.
 25. Morales H, Alfaro D, Martinot C, et al. MR spectroscopy of intracranial tuberculomas: a singlet peak at 3.8 ppm as potential marker to differentiate them from malignant tumors. *Neuroradiol J* 2015;28:294–302.
 26. Opstad KS, Provencher SW, Bell BA, et al. Detection of elevated glutathione in meningiomas by quantitative in vivo ¹H MRS. *Magn Reson Med* 2003;49:632–637.
 27. Panigrahy A, Krieger MD, Gonzalez-Gomez I, et al. Quantitative short echo time ¹H-MR spectroscopy of untreated pediatric brain tumors: preoperative diagnosis and characterization. *AJNR Am J Neuroradiol* 2006;27:560–572.
 28. Luthra G, Parihar A, Nath K, et al. Comparative evaluation of fungal, tubercular, and pyogenic brain abscesses with conventional and diffusion MR imaging and proton MR spectroscopy. *AJNR Am J Neuroradiol* 2007;28:1332–1338.
 29. Siegal JA, Cacayorinb ED, Nassif AS, et al. Cerebral mucormycosis: proton MR spectroscopy and MR imaging. *Magn Reson Imaging* 2000;18:915–920.
 30. Danielsen ER, Ross B. An introduction to clinical cases. In: Danielsen ER and Ross B (eds) *Magnetic resonance spectroscopy diagnosis of neurological diseases* Boca Raton, FL: CRC Press, 2018, pp.45–52.
 31. Kimura T, Sako K, Gotoh T, et al. In vivo single-voxel proton MR spectroscopy in brain lesions with ring-like enhancement. *NMR Biomed* 2001;14:339–349.
 32. Kuesel AC, Donnelly SM, Halliday W, et al. Mobile lipids and metabolic heterogeneity of brain tumours as detectable by ex vivo ¹H MR spectroscopy. *NMR Biomed* 1994;7:172–180.
 33. Qi ZG, Li YX, Wang Y, et al. Lipid signal in evaluation of intracranial meningiomas. *Chin Med J (Engl)* 2008;121:2415–2419.
 34. Lai PH, Weng HH, Chen CY, et al. In vivo differentiation of aerobic brain abscesses and necrotic glioblastomas multiforme using proton MR spectroscopic imaging. *AJNR Am J Neuroradiol* 2008;29:1511–1518.
 35. Shino A, Nakasu S, Matsuda M, et al. Noninvasive evaluation of the malignant potential of intracranial meningiomas performed using proton magnetic resonance spectroscopy. *J Neurosurg* 1999;91:928–934.
 36. Lehnhardt FG, Bock C, Röhn G, et al. Metabolic differences between primary and recurrent human brain tumors: a ¹H NMR spectroscopic investigation. *NMR Biomed* 2005;18:371–382.
 37. Akutsu H, Matsumura A, Isobe T, et al. Chronological change of brain abscess in (¹H) magnetic resonance spectroscopy. *Neuroradiology* 2002;44:574–578.
 38. Poptani H, Gupta RK, Jain VK, et al. Cystic intracranial mass lesions: possible role of in vivo MR spectroscopy in its differential diagnosis. *Magn Reson Imaging* 1995;13:1019–1029.
 39. Pinzariu O, Georgescu B, Georgescu CE. Metabolomics – a promising approach to pituitary adenomas. *Front Endocrinol (Lausanne)* 2018;9:814.
 40. Krishnamoorthy T, Radhakrishnan VV, Thomas B, et al. Alanine peak in central neurocytomas on proton MR spectroscopy. *Neuroradiology* 2007;49:551–554.
 41. Chuang MT, Lin WC, Tsai HY, et al. 3-T proton magnetic resonance spectroscopy of central neurocytoma: 3 case reports and review of the literature. *J Comput Assist Tomogr* 2005;29:683–688.
 42. Majós C, Alonso J, Aguilera C, et al. Adult primitive neuroectodermal tumor: proton MR spectroscopic findings with possible application for differential diagnosis. *Radiology* 2002;225:556–566.